Chemical Models of Genetic Toggle Switches†

Patrick B. Warren‡,§ and Pieter Rein ten Wolde*,§,||

Unilever R&D, Port Sunlight, Bebington, Wirral CH63 3JW, United Kingdom, FOM Institute for Atomic and Molecular Physics, Kruislaan 407, 1098 SJ Amsterdam, The Netherlands, and Division of Physics and Astronomy, Vrije Universiteit, De Boelelaan 1081, 1081 HV Amsterdam, The Netherlands

Received: October 1, 2004; In Final Form: November 25, 2004

We study by mean-field analysis and stochastic simulations chemical models for genetic toggle switches formed from pairs of genes that mutually repress each other. To determine the stability of the genetic switches, we make a connection with reactive flux theory and transition state theory. The switch stability is characterized by a well-defined lifetime τ. We find that τ grows exponentially with the mean number $\bar{N}$ of transcription factor molecules involved in the switching. In the regime accessible to direct numerical simulations, the growth law is well-characterized by $\tau \approx \bar{N}^{\alpha} \exp(b\bar{N})$, where α and b are parameters. The switch stability is decreased by phenomena that increase the noise in gene expression, such as the production of multiple copies of a protein from a single mRNA transcript (shot noise) and fluctuations in the number of proteins produced per transcript. However, robustness against biochemical noise can be drastically enhanced by arranging the transcription factor binding domains on the DNA such that competing transcription factors mutually exclude each other on the DNA. We also elucidate the origin of the enhanced stability of the exclusive switch with respect to that of the general switch; while the kinetic prefactor is roughly the same for both switches, the "barrier" for flipping the switch is significantly higher for the exclusive switch than that for the general switch.

1. Introduction

In an organism, genes can be turned on or off by the binding of proteins to regulatory sites on the DNA in the vicinity of the starting point for transcription.[1] The proteins are known as transcription factors, and the DNA binding sites are known as operators. The process is an example of gene regulation. Transcription factors can turn genes off by stereochemical blockage of the binding of RNA polymerase (RNAp), or they can turn genes on by cooperative binding (recruitment) of RNAp.[1]

Since transcription factors are proteins, they are coded for elsewhere on the genome. This means that transcription factors can regulate the production of other transcription factors or indeed can regulate their own production. A highly complex network of biochemical reactions can be built up, capable, in principle, of solving arbitrarily complex computational problems.[2,3] The network is interfaced to the outside world by, for example, signaling cascades from receptor proteins or by specific interactions between transcription factors and small molecules such as metabolites. In this way, even relatively simple organisms such as *E. coli* can perform fairly complex computations such as integrating different environmental signals. In higher organisms, gene regulatory networks lie at the heart of cell differentiation and developmental pathways.

Genetic toggle switches are an informative paradigm in this context.[4,5] They are regulatory constructs that select between two possible stable states, representing, for example, differentiation between two developmental pathways. Perhaps the simplest kind of switch is one that is constructed from a pair of genes that mutually repress each other, as indicated in Figure 1. The switch of λ-phage in *E. coli* is a naturally occurring example, which has been studied in much detail.[4,6−8] Another well-known example is that of the human herpesvirus 3 (chickenpox or varicella−zoster virus), which has a pathogenesis that is remarkably similar to λ-phage; the virus lies dormant after the initial infection but can be triggered to reemerge much later as shingles (herpes zoster). Synthetic toggle switches have also been constructed in vivo.[9]

Genetic switches are usually flipped by external signals. In the λ-phage, for example, the switch is initially in the dormant (lysogenic) state but can be flipped into the active (lytic) state by the presence of the bacterial protein RecA. Such an induction event occurs when the cell starts to produce RecA to repair DNA damage as a result of, for example, a burst of UV light.

Importantly, genetic switches are often so stable that they remain in one state until the external trigger flips the switch. In wild-type λ-phage, spontaneous flips are extremely rare, occurring at a rate of perhaps as low as one spontaneous flip in 10^{12} s.[8] An important question, therefore, is this: what are the design principles that allow the switch to attain such extreme stability in the presence of fluctuations and biochemical noise? This question is particularly relevant, because detailed modeling has suggested that the stability of λ-phage cannot be explained on the basis of our current understanding.[8]

We have recently shown that mutual exclusion of competing transcription factors can drastically enhance the stability of genetic switches.[10] Transcription factors can mutually exclude each other, if their operator sites (partially) overlap (Figure 1b). It appears that nature has exploited the functional benefit of this spatial arrangement of operators, since a recent statistical

* Author to whom correspondence should be addressed. Phone: +31-20-6081234. E-mail: tenwolde@amolf.nl.

† Part of the special issue "David Chandler Festschrift".

‡ Unilever R&D.

§ FOM Institute for Atomic and Molecular Physics.

|| Vrije Universiteit.

10.1021/jp045523y CCC: $30.25
Published on Web 01/21/2005

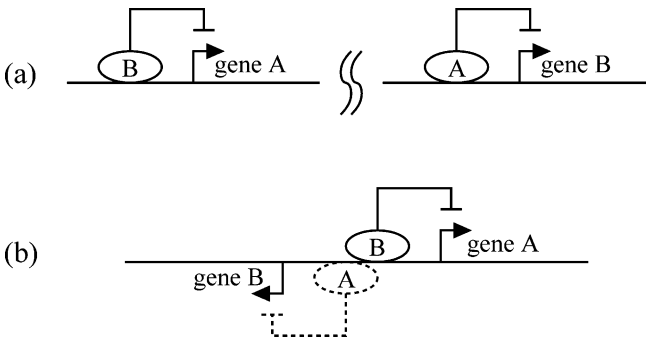

Figure 1. (a) A genetic toggle switch can be formed from a pair of genes that mutually repress each other's expression. (b) If the genes are transcribed on opposite strands of the DNA, then the upstream regulatory domains can overlap and interfere with one another. As a result, competing regulatory molecules mutually exclude each other. In the diagram, the horizontal lines represent the DNA, the solid arrows indicate the origin and direction of transcription for the indicated genes, the ovals indicate transcription factor binding sites, and the flat-headed arrows indicate that the transcription factor is a repressor for the target gene. In part b, the dashed oval and dashed flat-headed arrow represent the fact that for an exclusive switch binding of one transcription factor excludes binding of the other transcription factor.

analysis has revealed that this network motif of "overlapping operons" is over-represented in the bacterium *E. coli*.[11]

In this paper, we extend the analysis of ref 10 in several ways.[12] In the next section, we first describe the set of chemical reactions by which we model the genetic toggle switches (Figure 1). We then turn to a mean-field (chemical rate equation) analysis of the appearance of switching behavior. This mean-field analysis shows that the region of bistability is significantly larger for the exclusive switch than that for the general switch. To determine the lifetimes of the stable steady states of the switches, we have performed direct stochastic simulations; these are described in section 4. We then consider a number of refinements of the basic switch model. In particular, we explicitly take into account transcription and translation. We show that both "shot noise" and fluctuations in the number of proteins produced per mRNA transcript markedly decrease the switch stability. However, we again find that the exclusive switch is still orders of magnitude more stable than the general switch. In this paper, we also elucidate the origin of the enhanced stability of the exclusive switch with respect to that of the general switch; while the kinetic prefactor is roughly the same for both switches, the "free-energy" barrier for flipping is significantly higher for the exclusive switch than that for the general switch.[10] This underscores our earlier observation that mutual exclusion can drastically enhance the robustness of genetic switches to biochemical noise.[10] It also strongly supports the conjecture that regulatory control is one of the main evolutionary driving forces that shape the organization of genes and operons in the genome.[11]

2. Model Specification

Our starting point is a set of chemical reactions that model the processes involved in the toggle switches shown in Figure 1. As chemical species, we introduce a pair of transcription factors (TFs) that can exist as monomers, A and B, or multimers, A_n and B_m. The multimers are responsible for regulating gene expression and are allowed to bind to the genome at an operator site. Multimers are introduced in order to get sufficient cooperativity in the binding isotherms to make a genetic switch,[13] as described in more detail below. The state of the operator is represented by O, OA_n, etc., depending on the state of binding of the multimers. The chemical reactions are

$$nA \rightleftharpoons A_n \quad mB \rightleftharpoons B_m \ (k_f, k_b) \tag{1a}$$

$$O + A_n \rightleftharpoons OA_n \quad O + B_m \rightleftharpoons OB_m \ (k_{on}, k_{off}) \tag{1b}$$

$$OA_n + B_m \rightleftharpoons OA_nB_m \rightleftharpoons OB_m + A_n \ (k_{on}, k_{off}) \tag{1c}$$

$$O \rightarrow O + A \quad OA_n \rightarrow OA_n + A \ (k_A) \tag{1d}$$

$$O \rightarrow O + B \quad OB_m \rightarrow OB_m + B \ (k_B) \tag{1e}$$

$$A \rightarrow \varnothing \quad B \rightarrow \varnothing \ (\mu_A, \mu_B) \tag{1f}$$

The reactions in eq 1 account for, respectively, the formation of multimers, the binding of TF multimers to the operator, the expression of TF monomers, and the degradation of TF monomers. Repression of gene expression is implicit in eqs 1d and 1e; thus, A is expressed if and only if B_m is not bound, etc. Reaction rates are as indicated, and we define equilibrium constants for multimerization, $K_d = k_f/k_b$, and operator binding, $K_b = k_{on}/k_{off}$; in what follows, we assume that k_f and k_b and k_{on} and k_{off} are the same for species A and B.

While detailed and biologically faithful models can be constructed as has been done for the λ-phage switch,[6,8] the above model is intentionally as simple as possible. We believe that such an approach is as important as detailed biological modeling in elucidating the basic physical principles behind switches. Thus, for example, we have condensed the details of transcription and translation into single reaction steps in eqs 1d and 1e, governed by rate coefficients k_A and k_B. In a later section, we explore the possibility of refining the model at this point.

It should be noted, however, that the design of the network has to obey certain constraints. In particular, the TFs must bind cooperatively to the DNA to make a working switch.[13] In the present model, cooperativity is introduced through the binding of TF multimers rather than monomers.

In our model, the operator is in one of four states {O, OA_n, OB_m, OA_nB_m}. Interference between the upstream regulatory domains in the case of the exclusive switch in Figure 1b is modeled by removing eq 1c, thereby disallowing the state OA_nB_m. This is in the spirit of simplicity; strictly speaking, the effect is to modify the relative probabilities of the states. In our previous publication,[10] we also considered scenarios in which either one or both of the states OA_n and OB_m are disallowed, which we termed the partially and totally cooperative cases. However, these are biophysically unlikely and do not form very good switches; indeed, in the totally cooperative case no bistability is found at all.[10] We therefore do not consider these scenarios any further in the present paper.

3. Mean-Field Analysis

We first analyze the behavior of eq 1 using chemical rate equations. This plays the role of a mean-field theory for this problem since chemical rate equations describe the temporal evolution of the mean concentrations of the molecules. Switching behavior corresponds to the appearance of two distinct stable fixed points (attractors) in the space of concentration variables. For the general switch, the problem has been analyzed in detail by Cherry and Adler.[13] For the exclusive switch, a specific example has been studied by Kepler and Elston.[14] Our approach is a generalization of the analysis of Cherry and Adler.

Let us consider what happens for A. Write n_A for the number of A monomers in the cell etc., and let the cell volume be V_c.

In a steady state, the multimerisation reaction $n\mathrm{A} \rightleftharpoons \mathrm{A}_n$ is in equilibrium and

$$\left(\frac{n_{\mathrm{A}n}}{V_\mathrm{c}}\right) = K_\mathrm{d}\left(\frac{n_\mathrm{A}}{V_\mathrm{c}}\right)^n \tag{2}$$

Similarly the binding reaction $\mathrm{O} + \mathrm{A}_n \rightleftharpoons \mathrm{OA}_n$ is in equilibrium and

$$\left(\frac{n_{\mathrm{OA}_n}}{V_\mathrm{c}}\right) = K_\mathrm{b}\left(\frac{n_\mathrm{O}}{V_\mathrm{c}}\right)\left(\frac{n_{\mathrm{A}_n}}{V_\mathrm{c}}\right) \tag{3}$$

Now, n_O is the probability that the operator is in state O times the number of copies of the genome in the cell (usually assumed to be one), etc. Therefore

$$\frac{\mathrm{Prob}(\mathrm{OA}_n)}{\mathrm{Prob}(\mathrm{O})} = \frac{K_\mathrm{b}K_\mathrm{d}}{V_\mathrm{c}^{\,n}}[n_\mathrm{A}]^n \equiv x^n \tag{4}$$

where we have introduced x as a reduced concentration variable, equal to $(1/V_\mathrm{c})(K_\mathrm{b}K_\mathrm{d})^{1/n}$ times the number of monomers of A in the cell. Similarly, we introduce a reduced concentration variable y for the number of monomers of B.

From the totality of binding equilibria, we surmise that the probabilities of the operator states $\{\mathrm{O}, \mathrm{OA}_n, \mathrm{OB}_m, \mathrm{OA}_n\mathrm{B}_m\}$ are in the ratio $1{:}x^n{:}y^m{:}\gamma x^n y^m$ where we have covered off both switch construction possibilities by introducing a parameter γ such that

$$\gamma = \begin{cases} 1 \text{ (general switch)} \\ 0 \text{ (exclusive switch)} \end{cases} \tag{5}$$

The probability of the operator being in a state where A is expressed is therefore

$$f(x,y) = \frac{1 + x^n}{1 + x^n + y^m + \gamma x^n y^m} \tag{6}$$

and of being in a state where B is expressed is

$$g(x,y) = \frac{1 + y^n}{1 + x^n + y^m + \gamma x^n y^m} \tag{7}$$

For A, expression occurs at a rate k_A and degradation at a rate $\mu_\mathrm{A}n_\mathrm{A}$. It is convenient to define a reduced degradation rate

$$\tilde{\mu}_\mathrm{A} = \frac{V_\mathrm{c}}{(K_\mathrm{b}K_\mathrm{d})^{1/n}}\frac{\mu_\mathrm{A}}{k_\mathrm{A}} \tag{8}$$

If there is more than one copy of the genome in the cell, then we should additionally divide by the number of copies of the genome. A similar reduced degradation rate $\tilde{\mu}_\mathrm{B}$ is defined for B.

At a fixed point (a steady state), the rate of expression is equal to the rate of degradation (e.g., $k_\mathrm{A}f = \mu_\mathrm{A}n_\mathrm{A}$) for both TFs. Through use of the reduced concentrations and degradation rates defined above, the steady states are defined by

$$f(x,y) = \tilde{\mu}_\mathrm{A}x \quad g(x,y) = \tilde{\mu}_\mathrm{B}y \tag{9}$$

We see that the steady states only depend on $\tilde{\mu}_\mathrm{A}$ and $\tilde{\mu}_\mathrm{B}$.

The simplest way to proceed now is to consider the fixed points for the dynamical system

$$\dot{x} = f(x,y) - \tilde{\mu}_\mathrm{A}x \quad \dot{y} = g(x,y) - \tilde{\mu}_\mathrm{B}y \tag{10}$$

This is only an approximation to the full dynamics, since it assumes that TF binding is always in equilibrium. However, Cherry and Adler demonstrate under a mild restriction that the fixed points for eq 10 correspond to the possible fixed points of the full system. The mild restriction is that, under the full dynamics, if the concentration of one of the TFs is held fixed, then the concentration of the other TF should settle on a unique value. This holds for our switch problem.

Switching behavior corresponds to the existence of two stable fixed points for eq 10, separated by a third fixed point which is unstable in one direction, like a transition state. Thus, a test for switching behavior is whether the dynamical system in eq 10 admits an unstable fixed point that is unstable in one direction. From dynamical systems theory, this can be determined by considering the determinant of the stability matrix

$$\mathbf{M} = \begin{pmatrix} f_x - \tilde{\mu}_\mathrm{A} & f_y \\ g_x & g_y - \tilde{\mu}_\mathrm{B} \end{pmatrix} \tag{11}$$

where $f_x = \partial f/\partial x$, etc. The required test is that $\det \mathbf{M} < 0$ at the fixed point in question. At a fixed point, one can eliminate $\tilde{\mu}_\mathrm{A}$ and $\tilde{\mu}_\mathrm{B}$ between eqs 9 and 11. We find that $\det \mathbf{M} = (1/xy)\times D$ where we have introduced the discriminant function

$$D(x,y) = (f - xf_x)(g - yg_y) - xyg_xf_y \tag{12}$$

The sign of D mirrors the sign of $\det \mathbf{M}$ so that if $D < 0$ at a fixed point, then that fixed point is unstable in one direction. Moreover, for any point in the xy plane, D has a definite value independent of the values of $\tilde{\mu}_\mathrm{A}$ and $\tilde{\mu}_\mathrm{B}$. Thus, in the plane of reduced concentration variables, the nature of a fixed point is determined solely by its position. In particular, the region $D < 0$ contains all the unstable fixed points of the kind desired and only those kinds of fixed points. This region is bounded by the line $D = 0$.

Normally, one regards the parameters k_A, etc. as given, and one has to solve eq 9 for the position of any fixed points. However, if one knows a fixed point (x,y) in the plane of reduced concentration variables, then the corresponding reduced parameters are given by $\tilde{\mu}_\mathrm{A} = f/x$ and $\tilde{\mu}_\mathrm{B} = g/y$, from eq 9. The region $D < 0$ in the xy plane is therefore mapped to a region (a wedge) in the $\tilde{\mu}_\mathrm{A}\tilde{\mu}_\mathrm{B}$ plane. Figure 2 shows two examples. Note that the mapping from (x,y) to $(\tilde{\mu}_\mathrm{A},\tilde{\mu}_\mathrm{B})$ is triple-valued within the wedge, since for parameters where switching behavior occurs there are two stable fixed points in addition to the unstable fixed point.

An interesting analogy with a fluid−fluid demixing transition in a binary liquid mixture can be made at this point since both are examples of a cusp catastrophe.[15] In this analogy, $\tilde{\mu}_\mathrm{A}^{-1}$ and $\tilde{\mu}_\mathrm{B}^{-1}$ correspond to the chemical potentials of the two components and the wedge $D < 0$ to the region of spinodal instability. The cusp of the wedge in Figure 2b would correspond to the critical point.

We have analyzed in detail the situation for *dimerizing* switches, with $n = m = 2$. The details of this analysis are given in Appendix A. Figure 2 shows the regions in both the xy and $\tilde{\mu}_\mathrm{A}\tilde{\mu}_\mathrm{B}$ planes where switching behavior occurs. Clearly, there is a more extensive region of switching behavior in the $\tilde{\mu}_\mathrm{A}\tilde{\mu}_\mathrm{B}$ plane for the exclusive case compared to that of the general case. Thus, we conclude that, at least in mean-field theory, restricting the set of operator states can have a marked effect on the possibility to form a genetic switch.

4. Stochastic Simulations

While mean-field theory indicates the regions in parameter space where switching might occur, it has nothing to say about

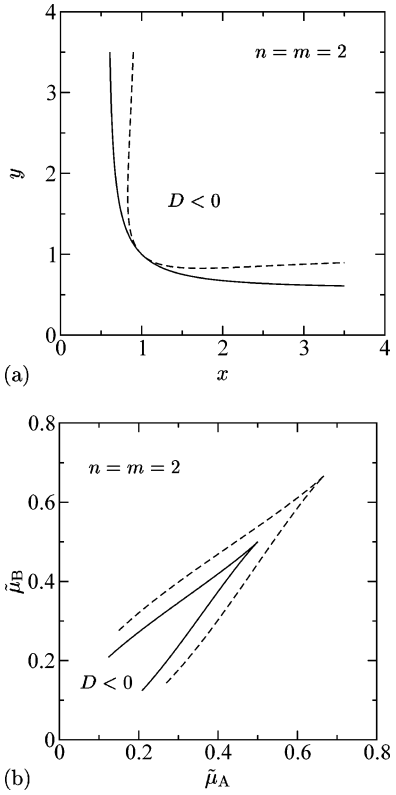

Figure 2. In mean-field theory, switching behavior is confined to a region (a) in the *xy* plane or equivalently to a wedge (b) in the $\tilde{\mu}_A\tilde{\mu}_B$ plane. Results are shown for dimerizing general (solid line) and exclusive (dashed line) switches.

TABLE 1: Rate Coefficients and Equilibrium Constants for a Representative Set of the Reactions Which Define the Baseline Model[a]

reaction	baseline		
$O \rightarrow O + A$	k_A	θ	
$A \rightarrow \varnothing$	μ_A	$(0.2-0.8)\theta$	
$2A \rightarrow A_2$	k_f	$5V_c\theta$	
$A_2 \rightarrow 2A$	k_b	5θ	$K_d = k_f/k_b = V_c$
$O + A_2 \rightarrow OA_2$	k_{on}	$5V_c\theta$	
$OA_2 \rightarrow O + A_2$	k_{off}	θ	$K_b = k_{on}/k_{off} = 5V_c$

[a]Here, V_c is the cell volume, and θ is used as a unit of (inverse) time.

the switch stability and the effects of number fluctuations in systems with a finite size. To address these problems, we therefore turn to a stochastic simulation of the chemical reactions in eq 1. This is done via the "Gillespie" algorithm,[16] which is a kinetic Monte Carlo scheme[17] to generate stochastic trajectories in the space of concentration variables appropriate to the chemical master equation.

Since these simulations are quite intensive, we focus again on the dimerizing switches and on the symmetry line $\mu_A = \mu_B = \mu$ and $k_A = k_B = \theta$. We additionally have to supply values for all the rate coefficients in eq 1. To do this, we let $\theta \approx 0.1-1$ s^{-1} be a unit of (inverse) time and use μ (the degradation rate) as the main control variable. As is the case with biological systems, real rate coefficients vary over quite a range of values. The baseline parameter set is biologically motivated, with expression being a slow step and binding equilibrium biased in favor of bound states. Rate coefficients for our baseline model for a representative set of reactions are given in Table 1. For comparison, literature values for λ-phage can be found in Arkin et al.,[6] in Aurell et al.,[7,8] and in Bundschuh et al.[18] The rate coefficients for bimolecular reactions, such as the forward dimerization and forward binding reactions, have units of volume divided by time. Since our concentrations are expressed as the number of molecules in the cell volume, the natural units for these rate coefficients are $V_c\theta$ where $V_c \approx 2\ \mu m^3$ ($1/V_c \approx 1$ nM) is the cell volume. For the baseline parameters, the mean-field theory predicts bistability for $\mu/\theta < \sqrt{5}/2 = 1.12$ for the general switch and $\mu/\theta < 2\sqrt{5}/3 = 1.49$ for the exclusive switch. The implementation of the Gillespie algorithm with concentrations expressed as the number of molecules in the cell is straightforward.

In the next section, we will first focus on the steady-state properties of both switches. In the subsequent section, we will address the dynamics of switching.

A. "Free-Energy" Landscapes. We monitor the total number of molecules of A and B in the cell, N_A and N_B. These include the monomers, the free dimers, and the bound dimers (e.g., eq 43). This is motivated primarily by the suggestion by Bialek that the switch lifetime is likely to be an exponential function of the number of molecules involved in the switching process.[19] Moreover, N_A and N_B are the relevant slow variables in the sense of Bundschuh et al.[18]

To demonstrate the appearance of switching, we can construct the probability distribution $P(N_A,N_B)$ for states in the N_AN_B plane. This is done by generating a sufficiently long Gillespie trajectory to obtain good coverage of all the interesting features of the probability distribution.[12] Figure 3 shows the main features for $\mu/\theta = 0.4$, for both the dimerizing general and exclusive switches with this direct method.

We see that switching appears as a double maximum in the probability distribution, and there is a transition state at a low number of molecules for both TFs; we *assume* here that the transition state corresponds to the saddle point in the "free-energy landscape" $-\log[P(N_A,N_B)]$. Table 2 contains the locations of the probability maxima and the transition state, comparing the Gillespie results with the mean-field theory fixed point solutions of the preceding section. The maxima are in quite good agreement with the mean-field fixed points, although there is some difference in the location of the saddle point. The first column in Table 3 shows the probability of reaching states with $N_A = N_B$ determined from Figure 3. This probability is an order of magnitude lower for the exclusive switch than that for the general switch, which indicates that the exclusive switch is more stable than the general switch.

B. Rate Constants. We now turn to the switch *dynamics*. Figure 4 shows a typical time series for $N_A - N_B$ for the dimerizing exclusive switch at $\mu/\theta = 0.4$. The appearance of the two switch states where one of the TFs is strongly repressed compared to the other one is clearly seen. These correspond to the probability maxima of Figure 3a. A switching event occurs when the roles of the two TFs flip spontaneously.

To elucidate the stability of the switches, we make a connection with the reactive flux method that has been pioneered by Bennett[20] and Chandler[21] and that is now widely used in the field of soft-condensed-matter physics.[22] We first define an order parameter, q, that serves as our reaction coordinate and measures the progress of flipping the switch from one state to the other. In what follows, we will take $q = N_A - N_B$. Furthermore, we define two characteristic functions that indicate in which state the system is in

$$h_A(q) = \Theta(q^* - q) \quad h_B(q) = \Theta(q - q^*) \qquad (13)$$

Here, Θ is the Heaviside function, $\Theta(x) = 0$ for $x < 0$ and

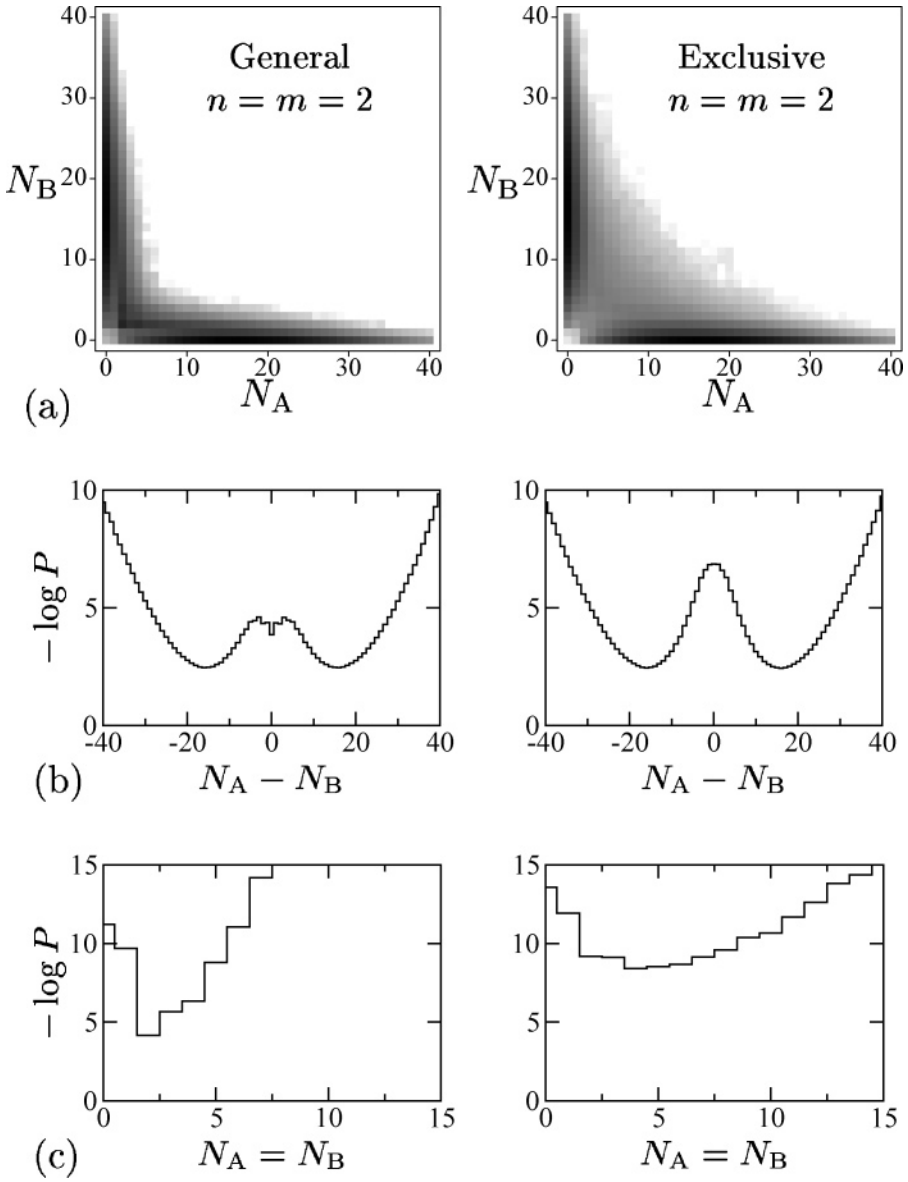

Figure 3. (a) Probabilities in the $N_A N_B$ plane constructed from trajectories of total duration $t\theta \approx 8 \times 10^6$, for general and exclusive switches, at $\mu/\theta = 0.4$. Gray scale is logarithmic from $P \leq 10^{-7}$ (white) to $P \geq 0.04$ (black). (b) Probabilities collapsed onto the $N_A - N_B$ line, plotted as a dimensionless "free energy" $-\log P$; the maximum at $N_A = N_B$ corresponds to the mean-field transition state. (c) Probabilities along the diagonal line $N_A = N_B$; the minimum in this section now corresponds to the mean-field transition state. It is seen that the saddle point of the exclusive switch is higher than that of the general switch. See also Table 2 for locations of the features in $P(N_A,N_B)$ and the barrier heights.

TABLE 2: Locations of Maxima and Transition States for $P(N_A,N_B)$ for Dimerizing General (DGS) and Exclusive (DES) Switches at $\mu/\theta = 0.4$ (Figure 3), Compared to Fixed Points from Mean-Field Theory (MFT, Section 3 and Appendix A)

		maximum		transition state
		N_A	N_B	$N_A = N_B$
DGS	Gillespie	15.0 ± 0.5	0	2 ± 1
($\gamma = 1$)	MFT	16.91	0.09	5.74
DES	Gillespie	15.0 ± 0.5	0	4 ± 1
($\gamma = 0$)	MFT	16.04	0.16	3.15

TABLE 3: Switching Kinetics[a]

	$P_0(q^*)$	$\tau\theta$	R/θ	$R(0^+)/\theta$	κ
DGS	$9(1) \times 10^{-3}$	$2.3(2) \times 10^3$	0.048(7)	0.24(1)	0.20(3)
DES	$0.92(1) \times 10^{-3}$	$8.0(5) \times 10^3$	0.14(1)	0.98(4)	0.14(1)

[a]The first column is the probability of reaching the top of the barrier from Figure 3, the second column is the lifetime from Figure 5, and the third column is kinetic prefactor defined to be $R = 1/(P_0(q^*)\tau)$. The fourth column is the mean escape rate $R(0^+)$ to $N_A > N_B$ from $N_A = N_B$ as determined from additional analysis of the simulations, and the final column is the transmission coefficient $\kappa = R/R(0^+)$. A figure in brackets after a result is an estimate of the error in the final digit of that result.

$\Theta(x) = 1$ for $x > 0$. It is natural to take for q^* the value that corresponds to the top of the "barrier" that separates the two stable steady sates. We have thus chosen $q^* = 0$ for both switches (Figure 3).

We now assume that we can make a separation of time scales.[22] In particular, we assume that there exists a time t that is longer than the time t_{trans} it takes for transient behavior to relax but shorter than the characteristic time t_{rxn} for making a transition from one state of the switch to the other. If this assumption holds, then we can coarse grain the switch as a two-state system. If the flipping on the time scale t_{rxn} is a Poisson process, then the relaxation of the switch is given by the

following expression

$$\frac{\overline{h_A(0)h_B(t)}}{\overline{h_A}} = \overline{h_B}(1 - \exp[-(k_{AB} + k_{BA})t]) \quad (14)$$

Here, the overbar denotes a time average; contributions to the average are weighted according to the stationary distribution of states. The expression on the left-hand side yields the probability that the switch is in state B at time t, given that initially it was in state A. If this time t is longer than t_{trans} and if there are no correlations between successive switching events on this time scale, then this correlation function should be given by the macroscopic expression on the right-hand side of the above equation, where k_{AB} and k_{BA} are the rate constants for flipping the switch in the forward and backward directions, respectively. The above relation thus only holds for $t > t_{trans}$.

It is instructive to take the time derivative in eq 14. This yields

$$\frac{\overline{h_A(0)\dot{h}_B(t)}}{\overline{h_A}} = \overline{h_B}(k_{AB} + k_{BA})\exp[-(k_{AB} + k_{BA})t] \quad (15)$$

If we now consider times t smaller than $t_{rxn} = 1/(k_{AB} + k_{BA})$ but larger than t_{trans} and exploit the detailed balance condition $\overline{h_B}/\overline{h_A} = k_{AB}/k_{BA}$, then we find

$$\frac{\overline{h_A(0)\dot{h}_B(t)}}{\overline{h_A}} = k_{AB} \quad (16)$$

This shows that the flux of trajectories from A to B should exhibit a plateau for times $t_{trans} < t < 1/(k_{AB} + k_{BA})$. Indeed, the macroscopic switching rate is precisely given by the constant flux of trajectories in this regime.

In general, however, it is useful to define a time-dependent rate constant

$$k_{AB}(t) = \frac{\overline{h_A(0)\dot{h}_B(t)}}{\overline{h_A}} \quad (17)$$

$$= \frac{\overline{\dot{q}(0)\delta(q(0) - q^*)\Theta(q(t) - q^*)}}{\overline{\Theta(q^* - q(t))}} \quad (18)$$

$$= \frac{\overline{\delta(q - q^*)}}{\overline{\Theta(q^* - q(t))}} \frac{\overline{\dot{q}(0)\delta(q(0) - q^*)\Theta(q(t) - q^*)}}{\overline{\delta(q - q^*)}} \quad (19)$$

$$= P_0(q^*)\overline{\dot{q}(0)\Theta(q(t) - q^*)}^* \quad (20)$$

$$= P_0(q^*)R(t) \quad (21)$$

The overline with the asterisk denotes an average over states at the top of the barrier.

It is seen that $k(t) = k_{AB}(t)$ is the product of two contributions. The first is $P_o(q^*)$, which is given by

$$P_0(q^*) = \frac{P(q^*)}{\sum_{-\infty}^{q^*} P(q)} \quad (22)$$

Here, $P(q)$ is the steady-state probability of finding the system with a reaction coordinate of size q. Noting that if $q < q^*$ the system is in the initial state, then it is clear that $P_o(q^*)$ is the probability of finding the system at the top of the barrier divided by the probability of finding it in the initial state. This quantity can be directly obtained from Figure 3 and is shown in Table 3.

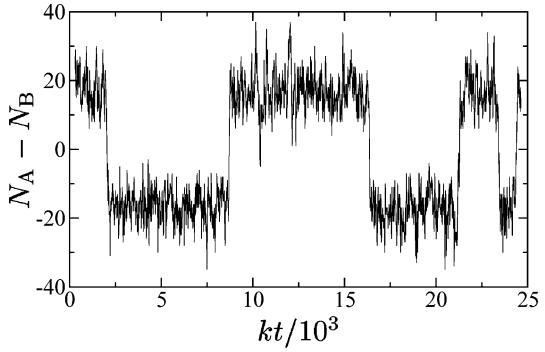

Figure 4. Typical time series for $N_A - N_B$ for the dimerizing exclusive switch at $\mu/\theta = 0.4$.

The second contribution to $k(t)$ is $R(t)$, which gives the average flux of trajectories at the top of the barrier. As explained in ref 21, the *initial* rate $k(t \rightarrow 0^+)$ corresponds to the approximation for the rate constant in the transition state theory of chemical reactions

$$k_{TST} = k(t \rightarrow 0^+) = P_0(q^*)\overline{\dot{q}(0)\Theta(\dot{q})} \quad (23)$$

Transition state theory assumes that all trajectories initially heading from the top of the barrier toward the final state will indeed end up in the final state and all trajectories initially heading toward the initial state will end up in the initial state. This assumption is only correct if no trajectories recross the barrier. In the present case, recrossing turns out to be quite significant, and as a result, $k(t)$ will be significantly lower than k_{TST}. It is conventional to express the reduction of $k(t)$ due to recrossings in terms of the transmission coefficient $\kappa(t)$, defined as

$$\kappa(t) \equiv \frac{k(t)}{k_{TST}} = \frac{R(t)}{R(0^+)} \quad (24)$$

where $R(0^+) = \overline{\dot{q}(0)\Theta(\dot{q})}^*$. We note that, just as $k_{AB}(t)$ exhibits a plateau value for $t_{trans} < t < t_{rxn} = 1/(k_{AB} + k_{BA})$, $\kappa(t)$ and $R(t)$ also reach a constant value on this time scale. We will simply refer to them as the transmission coefficient κ and kinetic prefactor R, respectively.

For many rare event problems in soft-condensed matter, it is not feasible to obtain the rate constant by calculating the correlation function $\langle h_A(0)h_B(t)\rangle$ in a long, brute-force simulation. To alleviate the rare event problem, a widely used approach is to first calculate the free-energy barrier $P_o(q^*)$ using umbrella sampling[23] and then compute the kinetic prefactor $R(t)$ by shooting off (molecular dynamics) trajectories from the top of the barrier.[20,21] However, the umbrella sampling technique in its conventional form relies on an energy functional and is therefore only applicable to systems that obey detailed balance. Biochemical networks are usually out of equilibrium and consequently lack detailed balance. In Appendix B, we show that the genetic toggle switches considered here also do not obey detailed balance. We can therefore not use the Bennett−Chandler approach.[20,21] Indeed, we have resorted to long, brute-force simulations to calculate the flipping rates for the toggle switches. To be more precise,[12] we have obtained the rate constant by fitting the correlation function $\overline{h_A(0)h_B(t)}/\overline{h_A}$ to its

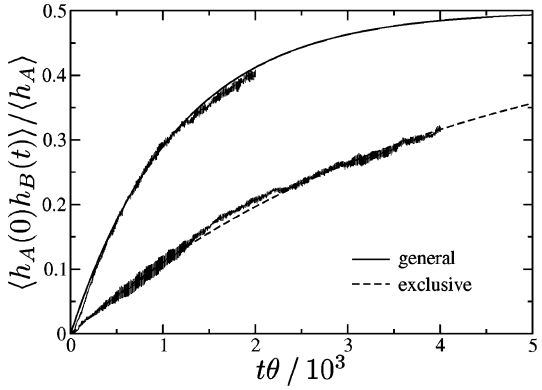

Figure 5. The cross correlation between the indicator functions $h_A = \Theta(q_A - q(t))$ and $h_B = \Theta(q(t) - q_B)$ allows an accurate determination of the switch lifetime. Results are shown for the general and exclusive switches at $\mu/\theta = 0.4$, with $-q_A = q_B = 5$. The lines are fits to eq 14 in the form $\langle h_A(0)h_B(t)\rangle/\langle h_A\rangle = (1 - \exp[-2t/\tau])/2$. Table 3 contains the corresponding values of τ.

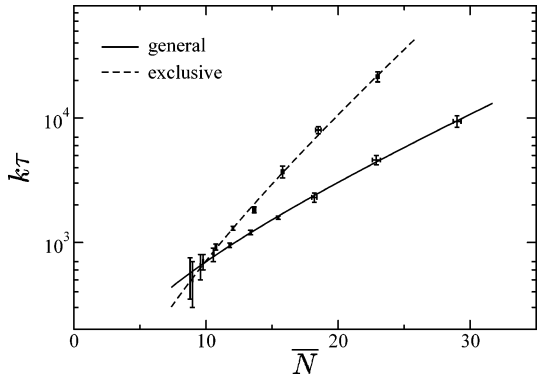

Figure 6. Switch lifetime as a function of the mean number of the most-expressed TF. The exclusive switch becomes orders of magnitude more stable than the general switch at high numbers of the expressed TF. The lines are fits to $\tau \approx \bar{N}^{\alpha} \exp(b\bar{N})$ as discussed in the text.

macroscopic expression as given by eq 14; for the symmetric switches considered here, $k_{AB} = k_{BA} = 1/\tau$, where τ is the lifetime of the stable steady state. In practice, to reduce noise in the correlation function, we excise a window of states around q^* and define $h_A = \Theta(q_A - q(t))$ and $h_B = \Theta(q(t) - q_B)$ where $q_A < q^*$ and $q_B > q^*$. Most of our calculations have been performed for $-q_A = q_B = 5$, but we find that, as expected, our results are insensitive to the precise values chosen, provided that the system is well into the bistable regime where there is a good separation of time scales. Figure 5 shows typical correlation functions.

In Figure 6, we show the switch lifetime $\tau = 1/k_{AB}$ ($= 1/k_{BA}$ for the symmetric switches) as a function of the mean value of the most-expressed transcription factor, defined to be the time average

$$\bar{N} = \overline{\max(N_A, N_B)} \tag{25}$$

We were motivated to examine τ as a function of $\bar{N}$ rather than μ by a conjecture due to Bialek, namely, that the switch lifetime may grow exponentially with the number of molecules involved in the switching process.[19]

We see that τ does grow extremely rapidly with $\bar{N}$, which is the basic reason extremely stable switches can be built with only a few hundred expressed proteins. Our simulations cover $10 \lesssim \bar{N} \lesssim 30$, but if we extrapolate our results to $\bar{N} \approx 100$, then $\tau\theta \approx 10^7$ for the general switch but $\tau\theta \approx 10^{11}$ for the exclusive switch. In the latter case, this corresponds to lifetimes measured in decades. Such extremely long lifetimes have been reported for λ-phage.[8] Equally important, Figure 6 is a dramatic confirmation that the switch construction has a marked influence on stability. The exclusive switch lifetime grows much more rapidly with the mean copy number than the general switch lifetime.

The dependence of τ on $\bar{N}$ can be fit to a functional form suggested by analysis of a related problem, namely, that of switching between broken symmetry phases in a driven diffusive model.[24,25] The fit is to $\tau\theta = A\bar{N}^{\alpha} \exp(b\bar{N})$, where $A = 50.4$, $\alpha = 0.72$, and $b = 0.097$ for the general switch and $A = 7.32$, $\alpha = 1.16$, and $b = 0.19$ for the exclusive switch. This fit gives quantitative support to Bialek's conjecture but additionally indicates that there is a (small) logarithmic correction in $\bar{N}$.

Table 3 shows the barrier heights $P_o(q^*)$ computed from the direct numerical simulations of $P(N_A,N_B)$. We can now obtain the kinetic prefactor R by dividing the rate constant $k_{AB} = 1/\tau$ by $P_o(q^*)$; $R = k_{AB}/P_o(q^*)$, see also eq 21. We find that the underlying barrier-crossing rate $R/\theta \approx 0.05-0.15$ is a (small) fraction of θ, which corresponds to the time scale for gene expression, Table 1. In fact, for the general switch, the kinetic prefactor R is significantly lower than the slowest reaction in the system, which is the degradation reaction with $\mu/\theta = 0.2-0.8$. Since R can be interpreted as the rate at which the barrier is crossed (i.e., the flux of trajectories at the top of the barrier), it is clear that crossing the barrier typically involves a large number of protein synthesis and degradation steps.

We have also directly computed from the Gillespie trajectories the distribution of escape times from the dividing surface $N_A = N_B$ to states with $N_A \neq N_B$. We find that for both kinds of switches, the escape time distribution is quite well approximated by a Poisson distribution with a characteristic lifetime $\tau_{\leftrightarrow}$. Since the switches are symmetric, this means we can define the escape rate to one side (e.g., to $N_A > N_B$) to be $R(0^+) = {}^1/_2\tau_{\leftrightarrow}$. Estimates for $R(0^+)$ from the Poisson distribution fit are shown in the fourth column in Table 3. The ratio of the barrier-crossing rate to the one-sided escape rate is the transmission coefficient, $\kappa = R/R(0^+)$. As Table 3 shows, the transmission coefficient for both kinds of switch is 10−20%. This shows that the barrier crossing is quite diffusive. In other words, a typical transition path between the two stable regions crosses and recrosses the top of the barrier $N_A = N_B$ several times before committing to one of the stable basins. This is in accord with our findings on the statistics of $q = 0$ crossing times reported previously.[10] It is also consistent with the observation that a typical transition path involves many protein synthesis and degradation reactions.

Finally, Figure 7 shows how $\bar{N}$ depends on μ. Since the system spends most of the time near a stable state, the average in eq 25 is dominated by the number of molecules in the stable states. As such, the time average can be compared to the stable fixed point in mean-field theory (Appendix A). Further, in the stable steady states both switches should behave very similarly. Figure 7 shows that while $\bar{N}$ is indeed nearly the same for the two switches it also lies systematically a little above the mean-field-theory prediction. We have, however, not explored this small deviation in detail.

5. Beyond the Baseline Model

We now consider the effects of varying parameters away from the baseline set and changing some other aspects such as introducing a more detailed representation of transcription and translation. Switch stability is generally unaffected by variation of the kinetic rates that do not alter the mean copy number of the TFs. What does have an effect, as we shall see, are

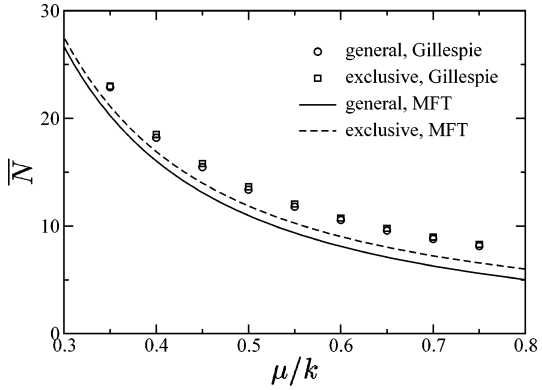

Figure 7. Mean copy number of the most-expressed TF, as a function of the degradation rate, for both kinds of switches and baseline parameters (Table 1). "Gillespie" refers to the results of the stochastic simulations and "MFT" refers to those of the mean-field analysis described in section 3.

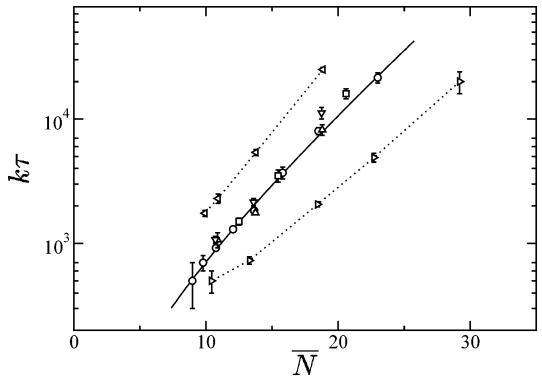

Figure 8. Switch lifetime for the dimerizing exclusive switch as some of the baseline kinetic parameters are varied. Data are shown for baseline model (circles; Table 1), with the number of copies of the genome doubled and expression rate halved (squares), with k_f and k_b doubled (up triangles), with k_{on} and k_{off} doubled (down triangles), with $k_{on} = 10V_c\theta$ and, as before, $k_{off} = \theta$ (left triangles), and with $k_{on} = 2V_c\theta$ and, as before, $k_{off} = \theta$ (right triangles); see Table 1 for the meaning of the rate constants. The solid line is the fit to the baseline data from Figure 6.

phenomena that increase the "shot noise" in expression. These include the generation of multiple copies of the TF from each mRNA transcript and stochastic fluctuations in the number of copies of the TF generated per mRNA transcript.

In this section, we give results for the dimerizing exclusive switch. We have repeated all the simulations for the dimerizing general switch, and we find that the same trends are recovered. We also find that the exclusive switch is *always* markedly more stable than the corresponding general switch, in a manner represented by Figure 6.

A. Varying Parameters Away from Baseline. Figure 8 shows that the switch lifetime is very insensitive to variations away from the baseline kinetic parameters that do not affect the mean-field steady states. If, however, we vary the kinetic parameters such that the mean-field steady states are changed, then we do see a systematic change in the switch stability. For instance, the switch stability is enhanced if the binding equilibrium is moved in favor of bound TF by increasing k_{on} (the rate of binding to DNA). This is because the number of molecules of each TF at the point where switching just starts decreases as $K_b = k_{on}/k_{off}$ increases (see eq 44), and thus at fixed $\bar{N}$ we are effectively moving deeper into the bistable region. This leads to a more stable switch. Thus, stability can be increased either by using an exclusive switch or by increasing

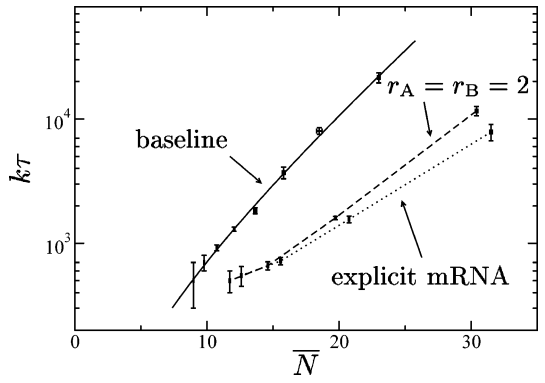

Figure 9. Switch stability is degraded if multiple copies of the TF are produced in each expression reaction; in this case, the number of copies is $r_A = r_B = 2$ (eq 26). In a model that includes explicit mRNA production (as described by eq 27), then even if on average only *one* TF is produced per transcript, the stability is similarly degraded by fluctuations about the mean. "Baseline" refers to the baseline model described in Table 1.

the binding affinity of the transcription factors or both. However, our results, comparing Figure 6 with Figure 8, suggest that the scaling of stability with the number of molecules is more favorable for the exclusive switch than for the general switch.

B. Effect of Messenger RNA. We have condensed the various steps in gene expression into single "expression reactions" in eqs 1d and 1e. In reality, however, many steps are involved. We now analyze these steps in more detail. Recall that the genetic information is first *transcribed* into messenger RNA (mRNA), then *translated* into proteins by ribosomes. It is often the case that several copies of the protein can be generated from one mRNA transcript. In the simplest way, we can capture this by replacing eqs 1d and 1e by versions in which r copies of each transcription factor are generated from each mRNA transcript, thus

$$\mathrm{O} \rightarrow \mathrm{O} + r_A\times\mathrm{A} \quad \mathrm{OA}_n \rightarrow \mathrm{OA}_n + r_A\times\mathrm{A}$$
$$\mathrm{O} \rightarrow \mathrm{O} + r_B\times\mathrm{B} \quad \mathrm{OB}_n \rightarrow \mathrm{OB}_n + r_B\times\mathrm{B} \qquad (26)$$

It is easy to see that nothing changes in mean-field theory provided that r_Ak_A and r_Bk_B are used in place of k_A and k_B. We have undertaken simulations for the case $r_A = r_B = 2$ and $k_A = k_B = \theta/2$, which in mean-field theory is identical to our baseline. However, as Figure 9 shows, the switch lifetime is decreased as a result of having TFs generated two at a time. The basic reason is that the "shot noise" in the expression reactions has increased.

Even if on average one TF is produced from each mRNA transcript, noise can arise from the fluctuations about this mean as we now discuss. To capture this, we explicitly include the generation and degradation of mRNA for the two TFs in the list of chemical reactions. The expression reactions in eqs 1d and 1e are replaced by the following reactions

$$\mathrm{O} \rightarrow \mathrm{O} + \mathrm{M_A} \quad \mathrm{OA}_n \rightarrow \mathrm{OA}_n + \mathrm{M_A}, (k'_A)$$
$$\mathrm{O} \rightarrow \mathrm{O} + \mathrm{M_B} \quad \mathrm{OB}_m \rightarrow \mathrm{OB}_m + \mathrm{M_B}, (k'_B)$$
$$\mathrm{M_A} \rightarrow \mathrm{M_A} + \mathrm{A} \quad \mathrm{M_A} \rightarrow \varnothing, (k''_A), (\mu'_B)$$
$$\mathrm{M_B} \rightarrow \mathrm{M_B} + \mathrm{B} \quad \mathrm{M_B} \rightarrow \varnothing. (k''_B), (\mu'_B) \qquad (27)$$

In these, M_A and M_B are the mRNA species, and the reactions represent the generation and degradation of mRNA and the translation of mRNA into TFs. We have introduced new rate

coefficients for the translation, transcription, and mRNA degradation steps.

In a steady state in mean-field theory, the rate of transcription balances the rate of mRNA degradation, and the mean number of mRNA transcripts is k'/μ' (we drop subscripts on k', k'', and μ' for clarity in this discussion). Each transcript produces TFs at a rate k''; hence, the overall rate of production of TF is $(k'/\mu')\times k''$. We conclude that the equivalent expression rate is

$$k = \frac{k'k''}{\mu'} \tag{28}$$

Going beyond mean-field theory, the statistics of this basic model for mRNA translation can be solved exactly.[26,27] Translation occurs at a rate k'' and degradation at a rate μ'; hence, the probability per unit time of either a translation or a degradation event taking place is $k'' + \mu'$. Given that an event has taken place, the probability that it was a translation event is $p = k''/(k'' + \mu')$, and the probability that it was a degradation event is $q = 1 - p = \mu'/(k'' + \mu')$. Therefore, the probability that r copies of the protein are generated before the mRNA transcript is degraded is $P_r = qp^r$. From this, all the statistics can be calculated. For instance, the mean number of TFs produced per transcript is $\langle r\rangle = \sum_{r=0}^{\infty} rP_r = p/q = k''/\mu'$, which agrees with the expectation from eq 28. Also, $\langle r^2\rangle = p/q^2$, so that the standard deviation divided by the mean is $\sqrt{q/p} = \langle r\rangle^{-1/2}$. Thus, there is considerable noise due to fluctuations in the number of proteins generated per transcript, and this noise is largest when the mean number of TFs produced per transcript is small.

To see the effect of this noise, we have implemented the additional reactions in eq 27 in our reaction schemes and again determined the switch lifetimes by direct simulation. Figure 9 shows the results for $k''_A = k''_B = 5k'_A = 5k'_B = \mu'_A = \mu'_B = 5\theta$. For these parameter values, $k''_Ak'_A/\mu'_B = k''_Bk'_B/\mu'_B = \theta$, and according to eq 28, such a system should be identical to our baseline. Moreover, since $k''_A/\mu'_A = k''_B/\mu'_B = 1$, there is on average one TF produced per mRNA transcript, so the "shot noise" associated with the mean number of TFs produced per transcript is the same as in the baseline model. However, the simulations clearly demonstrate that the additional noise due to fluctuations about this mean reduces the switch lifetime considerably.

C. Expression as a Multistep Process. As a second refinement to the model for gene transcription and translation, we now consider gene expression as a multistep process. We thus replace the single reaction $O \rightarrow O + A$ by a sequence of reaction steps

$$O \rightarrow O_1 \rightarrow O_2 \rightarrow O_3 \rightarrow ... \rightarrow O_n \rightarrow O + A \tag{29}$$

If there is only one intermediate stage, for example, O_1, this can be used to model the formation of an "open complex".[28] If there are multiple intermediate stages, this could represent the individual steps of the RNA polymerase that walks along the DNA or those of the ribosomes that walk along the mRNA. In some of the more detailed models of gene expression, all these intermediate steps are captured in detail.[6]

We can make a connection with the baseline model by computing the waiting time for the lumped reaction $O \rightarrow O + A$. Since the waiting times for the individual steps in eq 29 are independent statistical quantities, the waiting time for the whole sequence is the sum of the waiting times for the individual steps. In terms of reaction rates, $1/k = \sum 1/k_i$, where k is the rate of the lumped reaction and the k_i values are the rates of the intermediate steps.

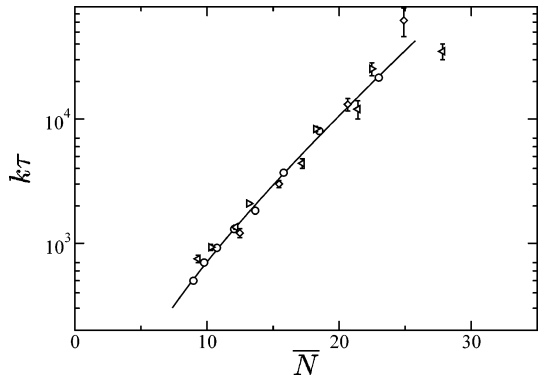

Figure 10. Compared to the baseline model (circles; Table 1), there is practically no effect on switch stability when one activation step is included (right triangles) or several are included (left triangles) as in eq 29 (see main text for details). There is also little change if the operator is split as in Figure 11 and eq 30 (diamonds). The line is the fit to the baseline data from Figure 6.

It follows that the waiting time distribution for the lumped reaction is not a Poisson distribution. Indeed the central limit theorem indicates that the lumped reaction will tend to have a Gaussian distribution of waiting times, effectively converging on a δ-function for a very large number of steps. Thus, the approximation that replaces eq 29 by $O \rightarrow O + A$ amounts to replacing the true non-Poisson distribution of waiting times by a Poisson distribution with the same mean.

We have tested the consequences of this assumption for two cases. In the first test, we have inserted a single intermediate stage in eq 29 to represent the formation of the open complex. The rates of the two steps were chosen to be $^5/_4\theta$ and 5θ so that formation of the open complex is the slow step. With this choice, the rate for the lumped reaction is the same as the baseline model. In the second test, we have inserted four intermediate stages in the reaction scheme, so that there are five intermediate reaction steps between O and O + A, to model, for example, the progressive stages of transcription. We have chosen the rates of these intermediate steps all equal to 5θ, so again the effective rate for the lumped reaction is the same as the baseline model. However, the sum of the variances for the individual steps is now 5 times smaller than the variance in the waiting time for the lumped reaction.

Figure 10 shows data for the dimerizing exclusive switch with these modifications. It shows that the switch stability is practically unaffected by the inclusion of the additional reaction steps. These results suggest that the precise waiting time statistics for these multistep reactions are less important for the switch stability than the statistics of the number fluctuations (as studied in considerable detail in the preceding section). This is perhaps not so surprising, since the activation process to flip the switch must proceed by multiple coincidences of the "right" expression or degradation events (see also discussion on kinetic prefactor R in section 4.2), and so the detailed waiting time statistics of the individual reaction steps appear to be unimportant.

D. Can the Operator be Split? The basic premise of the exclusive switch is that the binding of one TF excludes the binding of the other TF. While it is natural to think of this in terms of a diverging pair of genes on opposite strands of the DNA as shown in Figure 1b, it is also possible to achieve the same effect by having each TF prevent the binding of the other TF at separated operators on the DNA. An exclusive switch with such a "split" arrangement is shown in Figure 11. This arrangement is interesting because for each gene one TF

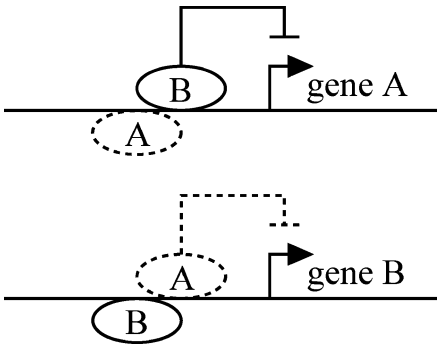

Figure 11. A "split" exclusive switch can be built out of distinct operators provided each TF blocks the other TF from binding at each operator site. The diagram corresponds to eq 30 in the text.

regulates expression by acting as a repressor but the other TF acts only indirectly by preventing binding of the repressor TF.

We can set up a system of chemical reactions to model the split operator case as follows. Suppose that O_A and O_B denote the operator sites for the genes that code for A and B, respectively. Then the set of reactions is

$$\begin{aligned} O_A + A_n &\rightleftharpoons O_A A_n \quad O_A + B_m \rightleftharpoons O_A B_m \ (k_{on}, k_{off}) \\ O_B + A_n &\rightleftharpoons O_B A_n \quad O_B + B_m \rightleftharpoons O_B B_m \ (k_{on}, k_{off}) \\ O_A &\rightarrow O_A + A \quad O_A A_n \rightarrow O_A A_n + A \ (k_A) \\ O_B &\rightarrow O_B + B \quad O_B B_m \rightarrow O_B B_m + B \ (k_B) \end{aligned} \tag{30}$$

plus the multimerization and degradation reactions from eq 1. This set of reactions describes the split analogue of the exclusive switch. In mean-field theory, this model is identical to the standard case. We have simulated this model and indeed find that there is little alteration to the switch stability, as shown in Figure 10.

We conclude that it is the exclusive nature of the TF binding that makes the exclusive switch markedly more stable than the general case. This can be achieved by overlapping the operator sites of genes that are arranged in a divergent manner and (thus) on opposite strands of the DNA as in Figure 1b or by the pure exclusive binding arrangements of Figure 11. It appears, however, that nature has taken advantage of the elegance of the former scenario; in *E. coli*, there are a significantly large number of diverging gene pairs with overlapping operator sites.[11]

6. Discussion

A genetic switch is inherently stochastic, because of the molecular character of its components. Our simulations demonstrate that the stability of a genetic switch can be strongly influenced by its construction. If the competing transcription factors mutually exclude each other at the operator regions, then the switch stability is markedly enhanced. Mutual exclusion of competing regulatory molecules can be obtained by overlapping operons, a network motif that we have recently identified in a statistical analysis of the gene regulatory network of *E. coli*.[11]

The basic conclusion that mutual exclusion of competing regulatory molecules can strongly enhance the stability of biochemical networks is robust. Nevertheless, the switch stability is influenced by phenomena that increase the noise in gene expression. Such phenomena include the generation of multiple copies of a transcription factor from the same mRNA transcript as well as intrinsic noise arising from the fluctuations in the numbers of proteins produced from a transcript.

When expressed as a function of the number of molecules involved in switching, the switch stability is characterized by a well-defined lifetime τ that grows exponentially with the mean number, $\bar{N}$, of the transcription factors that are involved in the switching. In the regime accessible to direct numerical simulations, the growth law is well-characterized by $\tau \approx \bar{N}^{\alpha} \exp(b\bar{N})$, where α and b are parameters.

Whereas we have investigated a number of details that might affect switch stability, we have left out some considerations that might additionally be important. Foremost among these is the influence of cell division and the cell cycle. Other effects such as fluctuations in the availability of RNA polymerase and ribosomes might also have an influence on switch stability. Another aspect that should be investigated is the response of the switch to a perturbation, in other words how one might toggle a switch by introducing a pulse of some kind. We leave all these questions to future work.

The rapid increase of the switch stability with the number of expressed transcription factors presents a fundamental limitation to the use of direct simulation to compute the switch lifetime. This provokes the question: is there a smarter way to compute the switch stability for long-lived switches? Such simulation methods would generally be useful since the characterization of rare events remains a key challenge in computational systems biology.[29] In the field of soft-condensed-matter physics, numerical techniques, such as the reactive flux method[20,21] and transition path sampling,[30] have been developed that make it possible to simulate rare events such as crystal nucleation, protein folding, and chemical reactions. Biochemical networks, however, differ fundamentally from these problems. In the former problems, the stationary distribution of states is usually known beforehand. Indeed, these systems typically obey detailed balance. In contrast, our genetic circuits, like most biochemical networks, do not satisfy detailed balance. This means that the stationary distribution of states is not known a priori. As a result, numerical techniques developed to tackle rare events in the field of soft-condensed-matter physics cannot straightforwardly be transposed to biochemical networks. Recently, we have developed a new numerical technique, called forward flux sampling,[31] that does not rely upon prior knowledge of the stationary distribution of states. The scheme is easily applicable to a wide variety of biochemical switches, such as that of bacteriophage λ, and makes it possible to calculate rates of switching and to identify pathways for switching. The technique should therefore lead to a better understanding of these rare but important events in biology.

Acknowledgment. We thank Rosalind Allen and Daan Frenkel for useful discussions and for a critical reading of the manuscript and Martin Evans for drawing our attention to the work on driven diffusive systems. We thank Nick Buchler for drawing our attention to the split operator arrangement shown in Figure 11. We are also grateful to the hospitality of the Kavli Institute for Theoretical Physics in Santa Barbara, where part of the work was carried out. This research was supported in part by the National Science Foundation under Grant No. PHY99-07949. This work is supported by the Amsterdam Centre for Computational Science (ACCS). The work is part of the research program of the "Stichting voor Fundamenteel Onderzoek der Materie" (FOM), which is financially supported by the "Nederlandse Organisatie voor Wetenschappelijk Onderzoek" (NWO).

Appendix A: Mean-Field Theory for Dimerizing Switches

Here are the explicit results of the mean-field (chemical kinetics) analysis for the dimerizing switches. First, consider the general switch. For this case, $\gamma = 1$, and eqs 6 and 7 simplify to $f = 1/(1 + y^2)$ and $g = 1/(1 + x^2)$. The discriminant equation $D = 0$ solves to

$$y^2 = \frac{x^2 + 1}{3x^2 - 1} \tag{A1}$$

and requires $x > 1/\sqrt{3} \approx 0.577$ for solutions. The cusp of the wedge in the $\tilde{\mu}_A\tilde{\mu}_B$ plane lies at the point $\tilde{\mu}_A = \tilde{\mu}_B = {}^1/_2$ and corresponds to the point $x = y = 1$ on the line $D = 0$.

For the exclusive switch ($\gamma = 0$), eqs 6 and 7 give $f(x,y) = (1 + x^2)/(1 + x^2 + y^2)$ and $g(x,y) = f(y,x)$. The discriminant equation $D = 0$ now solves to

$$y^2 = \frac{\pm\sqrt{x^8 + 14x^6 + 25x^4 - 24x^2} - x^4 - 5x^2 + 2}{2(x^2 - 1)} \tag{A2}$$

This requires $x > \sqrt{(3\sqrt{17} - 11)/\sqrt{2}} \approx 0.827$ for solutions, at which point $y = \sqrt{3} \approx 1.73$. The curve for $x > 1$ corresponds to the positive sign; one can show that the curve for $x < 1$ can be generated by reflecting the curve for $x > 1$ through the line $x = y$ (the curve passes through $x = y = 1$). Also, $y \to 1$ as $x \to \infty$. The cusp of the wedge in the $\tilde{\mu}_A\tilde{\mu}_B$ plane lies at the point $\tilde{\mu}_A = \tilde{\mu}_B = {}^2/_3$, again corresponding to the point $x = y = 1$ on the line $D = 0$.

We now describe the mean-field fixed points for dimerizing exclusive and general switches along the symmetry line $\mu_A = \mu_B = \mu$ and $k_A = k_B = \theta$. We assume there is one copy of the genome in the cell. The reduced degradation rate is

$$\tilde{\mu} = \frac{V_c}{\sqrt{K_b K_d}}\frac{\mu}{\theta} \tag{A3}$$

For the general switch, eq 9 is

$$\frac{1}{1 + y^2} = \tilde{\mu}x \quad \frac{1}{1+x^2} = \tilde{\mu}y. \tag{A4}$$

The stable fixed points are

$$(x,y) = \frac{1 \pm \sqrt{1 - 4\tilde{\mu}^2}}{2\tilde{\mu}} \tag{A5}$$

where $x > y$ if the positive sign is taken for x. We see that $\tilde{\mu} < {}^1/_2$ is required as found earlier (Figure 2). The unstable fixed point is

$$x = y = \frac{u - 12\tilde{\mu}^2/u}{6\tilde{\mu}} \tag{A6}$$

where

$$u^3 = 108\tilde{\mu}^2 + 12\tilde{\mu}^2\sqrt{81 + 12\tilde{\mu}^2} \tag{A7}$$

For the exclusive switch, eq 9 is

$$\frac{1 + x^2}{1 + x^2 + y^2} = \tilde{\mu}x \quad \frac{1 + y^2}{1 + x^2 + y^2} = \tilde{\mu}y \tag{A8}$$

The stable fixed points are

$$(x,y) = \frac{[1 - 2\tilde{\mu}^2 + \sqrt{1 + 4\tilde{\mu}^2} \pm \Delta]^{1/2}}{2\tilde{\mu}} \tag{A9}$$

where $x > y$ if the positive sign is taken for x, and

$$\Delta^2 = 2 - 12\tilde{\mu}^4 + 2(1 - 2\tilde{\mu}^2)\sqrt{1 + 4\tilde{\mu}^2} \tag{A10}$$

One can check that $\Delta^2 > 0$ requires $\tilde{\mu} < {}^2/_3$, as found earlier. The unstable fixed point is

$$x = y = \frac{1 + \upsilon + (1 - 6\tilde{\mu}^2)/\upsilon}{6\tilde{\mu}} \tag{A11}$$

where

$$\upsilon^3 = 1 + 45\tilde{\mu}^2 + 3\tilde{\mu}\sqrt{12 + 213\tilde{\mu}^2 + 24\tilde{\mu}^4} \tag{A12}$$

An expression for the total number of molecules of A in the cell that applies to both kinds of switches is given by

$$N_A = n_A + 2\,n_{A_2} + 2\,n_{OA_2} = \frac{xV_c}{\sqrt{K_b K_d}} + \frac{2x^2V_c}{K_b} + \frac{2(x^2 + \gamma x^2y^2)}{1 + x^2 + y^2 + \gamma x^2y^2} \tag{A13}$$

The total number of molecules of B is given by the same expression with x and y interchanged. This expression, together with the results above for the locations of the fixed points, is used to fill in the mean-field rows in Table 2. For both kinds of switches, $x = y = 1$ at the largest value of $\tilde{\mu}$ for which bistability occurs. Therefore at this point

$$N_A = N_B = \frac{V_c}{\sqrt{K_b K_d}} + \frac{2V_c}{K_b} + 2\frac{1 + \gamma}{3 + \gamma} \tag{A14}$$

We finally consider briefly the limit $\tilde{\mu} \to 0$, which is the limit of high expression and low degradation rates. In this limit, the stable fixed points for both exclusive and general switches converge with $x \approx 1/\tilde{\mu}$ and $y \approx \tilde{\mu}$ (or vice versa). However, the behavior of the unstable fixed point is $x = y$ and $x \approx \tilde{\mu}^{-1/3}$ for the general switch and $x = y$ and $x \approx 1/(2\tilde{\mu})$ for the exclusive switch.

Appendix B: Lack of Detailed Balance

We prove that the chemical master equation for the set of reactions in eq 1 cannot satisfy detailed balance. Recall that detailed balance implies that

$$W(1 \to 2)P_S(1) = W(2 \to 1)P_S(2) \tag{B1}$$

where "1" and "2" indicate any two states, $W(1 \to 2)$ and $W(2 \to 1)$ are the forward and backward transition rates between the states, and P_S is the steady-state probability distribution.[32] If detailed balance holds, then P_S is unique, and all other probability distributions move toward P_S. For many problems, P_S is known (eg, it is the Gibbs−Boltzmann distribution). The problem is then to find a set of W that satisfies detailed balance, thus guaranteeing that the dynamics has the correct equilibrium distribution. This is the case for Metropolis Monte Carlo schemes, for example. For the Gillespie algorithm or the chemical master equation, however, the W are prescribed, and we do not necessarily know P_S.

Without prior knowledge of P_S, it would seem difficult to determine from W alone whether a system obeys detailed

balance or not. However, Mukamel describes a useful test.[33] Consider any cycle of states {1, 2, 3, ..., k, 1}. A necessary and sufficient condition for the existence of detailed balance is that

$$W(1 \rightarrow 2)W(2 \rightarrow 3) \ldots W(k \rightarrow 1) = W(1 \rightarrow k)W(k \rightarrow k-1) \ldots W(2 \rightarrow 1) \quad \text{(B2)}$$

for all such cycles. To prove that a system does not obey detailed balance, it suffices to find a single counter example.

For our problem as formulated in eq 1, we can consider the following cycles. The product of the transition rates around the cycle starting at the state OB_2 is $k_{off} \times k_A \times k_{on} \times \mu_A$, which is

$$\begin{array}{ccc} OB_2 & \rightarrow & O + B_2 \\ \uparrow & & \downarrow \\ OB_2 + A & \leftarrow & O + B_2 + A \end{array} \quad \text{(B3)}$$

clearly positive. However, the product of the transition rates around the inverse cycle starting at the state OB_2 is

$$\begin{array}{ccc} OB_2 & \leftarrow & O + B_2 \\ \downarrow & & \uparrow \\ OB_2 + A & \rightarrow & O + B_2 + A \end{array} \quad \text{(B4)}$$

$0 \times k_{off} \times \mu_A \times k_{on}$, which clearly vanishes. Thus, the products of the transition rates are different for the two cycles, which proves that the corresponding master equation cannot obey detailed balance. If we examine the cycles in more detail, then we see that the binding, unbinding, and degradation steps are present in both the forward and the reverse cycles (albeit in a different order), so the key to the argument is the fact that the rate of expression of A is different for the genome states O and OB_2. Such a difference expresses the essence of transcriptional regulation in our system. It is clear that the same argument can be deployed whenever the appearance of a molecule in the system depends on the state of binding of some other molecules. This is very common, for instance, it applies whenever one has gene regulation by a transcription factor. Thus, lack of detailed balance would appear to be a generic feature of most realistic biochemical networks.

References and Notes

(1) Ptashne, M.; Gann, A. *Genes and Signals*; Cold Spring Harbor Laboratory Press: New York, 2002.

(2) Magnasco, M. O. *Phys. Rev. Lett.* **1997**, *78*, 1190.

(3) Eguia, M. C.; Ponce Dawson, S.; Mindlin, G. B. *Phys. Rev. E* **2002**, *65*, 047201.

(4) Ptashne, M. *A Genetic Switch: Phage Lambda and Higher Organisms*, 2nd ed.; Blackwell: Oxford, 1992.

(5) Ferrell, J. J. E. *Curr. Opin. Chem. Biol.* **2002**, *6*, 140.

(6) Arkin, A.; Ross, J.; McAdams, H. H. *Genetics* **1998**, *149*, 1633.

(7) Aurell, E.; Sneppen, K. *Phys. Rev. Lett.* **2002**, *88*, 048101.

(8) Aurell, E.; Brown, S.; Johanson, J.; Sneppen, K. *Phys. Rev. E* **2002**, *65*, 051914.

(9) Gardner, T. S.; Cantor, C. R.; Collins, J. J. *Nature* **2000**, *403*, 339.

(10) Warren, P. B.; ten Wolde, P. R. *Phys. Rev. Lett.* **2004**, *92*, 128101.

(11) Warren, P. B.; ten Wolde, P. R. *J. Mol. Biol.* **2004**, *342*, 1379.

(12) Our analysis also improves on ref 10 in a couple of ways. First, we now define $P(N_A,N_B)$ in Figure 3 to be a true time average, proportional to the total time the system spends in states with given values of N_A and N_B rather than simply proportional to the number of times the system visits states with given values of N_A and N_B. Second, we now calculate the switch lifetime from the correlation function in eq 14 as described in the main text rather than by analyzing the time Δt between crossings of the surface $N_A - N_B = 0$, as in ref 10. The latter method is error prone, as it interprets all fluctuations that take the system from a stable state to the dividing surface $N_A - N_B = 0$ as true crossing events; even the transient fluctuations that do not correspond to barrier-crossing events are counted as such. In contrast, in the method based upon the correlation function in eq 14, such events only contribute to the short-time noise; they do not affect the estimate for the rate constant.

(13) Cherry, J. L.; Adler, F. R. *J. Theor. Biol.* **2000**, *203*, 117.

(14) Kepler, T. B.; Elston, T. C. *Biophys. J.* **2001**, *81*, 3116.

(15) Gilmore, R. *Catastrophe Theory for Scientists and Engineers*; Dover: New York, 1981.

(16) Gillespie, D. T. *J. Phys. Chem.* **1977**, *81*, 2340.

(17) Bortz, A. B.; Kalos, M. H.; Lebowitz, J. L. *J. Comput. Phys.* **1975**, *17*, 10.

(18) Bundschuh, R.; Hayot, F.; Jayaprakash, C. *Biophys. J.* **2003**, *84*, 1606.

(19) Bialek, W. In *Advances in Neural Information Processing*; Leen, T. K., Dietterich, T. G., Tresp, V., Eds.; MIT Press: Cambridge, 2001, Vol. 13 (cond-mat/0005235).

(20) Bennett, C. H. In *Algorithms for Chemical Computations*; Christofferson, R. E., Ed.; American Chemical Society: Washington, DC, 1977.

(21) Chandler, D. *J. Chem. Phys.* **1978**, *68*, 2959.

(22) Chandler, D. *Introduction to Modern Statistical Mechanics*; Oxford University Press: New York, 1987.

(23) Torrie, G. M.; Valleau, J. P. *Chem. Phys. Lett.* **1974**, *28*, 578.

(24) Evans, M. R.; Foster, D. P.; Godrèche, C.; Mukamel, D. *Phys. Rev. Lett.* **1995**, *74*, 208.

(25) Godrèche, C.; Luck, J. M.; Evans, M. R.; Mukamel, D.; Sandow, S.; Speer, E. R. *J. Phys. A: Math. Gen.* **1995**, *28*, 6039.

(26) McAdams, H. H.; Arkin, A. *Proc. Natl. Acad. Sci., U.S.A.* **1997**, *94*, 814.

(27) Thattai, M.; van Oudnaarden, A. *Proc. Natl. Acad. Sci., U.S.A.* **2001**, *98*, 8614.

(28) Wagner, R. *Transcription Regulation in Prokaryotes*; OUP: Oxford, 2000.

(29) Rao, C. V.; Wolf, D. M.; Arkin, A. P. *Nature* **2002**, *420*, 231.

(30) Bolhuis, P. G.; Chandler, D.; Dellago, C.; Geissler, P. L. *Annu. Rev. Phys. Chem.* **2002**, *53*, 291.

(31) Allen, R. J.; Warren, P. B.; ten Wolde, P. R. *Phys. Rev. Lett.* **2005**, *94*, 018104.

(32) van Kampen, N. G. *Stochastic Processes in Physics and Chemistry*; Elsevier: Amsterdam, 2001.

(33) Mukamel, M. In *Soft and Fragile Matter*; Cates, M. E., Evans, M. R., Eds.; IOP Publishing: London, 2000.